Experimental Study of the Tubular Multiphase Catalyst

Philippe Cini and Michael P. Harold
Dept. of Chemical Engineering, University of Massachusetts, Amherst, MA 01003

A new type of multiphase catalyst is developed for transport-controlled, volatile-reactant-limited reactions: the tubular-supported ceramic membrane. A microporous, catalytically-impregnated γ-Al_2O_3 film (permeable membrane) coats the inside wall of a hollow, macroporous α-Al_2O_3 tube. The gas containing the volatile reactant flows through the tube core, and the liquid containing the nonvolatile and dissolved volatile reactants flows on the shell side. Reaction occurs in the film. Results using the hydrogenation of α-methylstyrene to cumene on Pd/Al_2O_3 reveal that the tubular catalyst compares favorably to conventional catalyst designs. The results demonstrate that the main benefit is the more efficient supply of the volatile reactant. Apparent activation energy analyses reveal that for catalyst temperatures below 40° C, the rate is kinetically-controlled and catalyst utilization nearly complete. A reduction in the activation energy above 45°C indicates the onset of transport limitations or heat effects. A comparison between the tubular catalyst and a fully-wetted pellet reveals rate increases by up to a factor of 20.

Introduction

Catalytic reactions between volatile and nonvolatile species are frequently carried out in the fixed-bed multiphase reactor. In this type of reactor, the gas and liquid phases are pumped cocurrently downward over a fixed bed of catalyst pellets. Mass transport limitations are problematic in these reactors. In liquid-filled catalyst pellets, the typically large ratio of diffusion to reaction times results in significant intraparticle mass transfer resistance. In addition, the liquid film covering the pellets constitutes an external mass transfer resistance to the supply of the volatile reactant. Moreover, the complex multiphase flows can be the root cause of many operational problems. In the trickling flow regime, liquid maldistribution and channelling lead to poor contacting of the catalyst. At sufficiently low liquid flow rates, the catalyst pellets become partially wetted. The combination of flow maldistribution or partial wetting, exothermic reaction heat, and a volatile liquid phase can lead to hot spots or zones in the reactor within which only a gas-phase catalytic reaction occurs. These hot spots can lead to catalyst sintering, and can initiate undesirable side reactions or a reactor runaway.

These disadvantages of the fixed-bed multiphase reactor have motivated us to develop a new type of reactor that has considerably simpler hydrodynamic features and improved mass and heat transport characteristics (Harold et al., 1989). The essential component of the reactor is a tubular-supported catalytic membrane. A hollow, macroporous ceramic (e.g., α-Al_2O_3) tube is coated on its inside wall with a thin, microporous ceramic (e.g., γ-Al_2O_3) film which serves as a permeable membrane. This ceramic membrane is impregnated with a catalytic component (e.g., precious metal). The two phases are then flowed in a segregated fashion: the liquid flows on the outside of the tube, whereas the gas flows in the core of the tube. Capillary forces cause the liquid to penetrate the pores of the support tube and membrane. Reaction between the dissolved volatile and nonvolatile reactants occurs in the catalytically impregnated membrane. Whether this is a gas-phase or liquid-phase catalytic reaction would depend on the heat of reaction, the liquid component volatilities, and other factors. The reactor is envisioned to consist of a vessel containing a bank of such catalytic tubes. Thus, the flow is relatively simple, which makes both the reactor design and operation considerably less complicated. A key improvement is also gained with respect to the mass transport features. The volatile reactant does not have to diffuse through a liquid film to reach the catalyst. This virtually eliminates the external mass transfer resistance on the gas side. Such partial wetting of the catalyst can lead to improve catalyst utilization and is called effectiveness enhancement (Harold and Ng, 1987; Funk et al., 1990).

Correspondence concerning this article should be addressed to M. P. Harold.
The present address of P. Cini: Westhollow Research Center, 3333 Highway 6 South, Houston, TX 77082.

Moreover, the intraparticle mass transfer resistance can be minimized by reducing the thickness of the tube wall and active layer. A previous modeling study showed that the tubular reactor outperforms the trickle-bed with regards to catalyst utilization for volatile-reactant-limited reactions (Harold et al., 1989).

Other pioneering studies have considered alternative designs to enhance the mass transfer in multiphase catalytic reactions. All of these designs segregated the gas and liquid flow. de Vos et al. (1982) converted a standard cross-flow heat exchanger into a supported Pd catalyst to carry out liquid-phase hydrogenations. The exchanger was made up of parallel porous calcium aluminum silicate plates reinforced by glass fibers. Gas and liquid streams were passed through adjacent passages. Overall effectiveness was higher than that obtained with the same reaction carried out in the trickle-bed packed with Pd/carbon catalyst. Other designs involved the use of polymeric hollow fibers (Yang et al., 1987) or a ceramic monolith (Hatziantoniou et al., 1982, 1984, 1986).

In the present work, we have three objectives. The first objective is to demonstrate that the tubular-supported catalytic membrane reactor can perform well and without any major operational problems. To simplify the design and analysis, a single-tube reactor is considered. The hydrogenation of α-methylstyrene on Pd/Al_2O_3 is selected as the test reaction, since it is representative of the large class of commercially-important, volatile-reactant-limited, mass-transfer-controlled, multiphase reactions.

The second objective is to study the reaction-transport interactions occurring in the reactor. To be identified are which of the two reactants is limiting and which process (i.e., reaction and transport) is rate-controlling for a given set of conditions. These identifications are essential for determining the operating conditions and reaction types for which this new reactor is best suited.

The third objective is to determine the performance advantages of this new design compared to a more conventional design. More specifically, our aim is to quantify the benefits gained from the partial wetting of the catalyst in the tubular-supported catalytic membrane configuration. We compare overall rates obtained with the tubular-supported catalytic membrane to those of a surface-shell, catalytically-impregnated pellet. The latter pellet, if fully wetted by the liquid, simulates the performance of a pellet in a trickle bed at sufficiently high liquid flow rates.

Catalyst Preparation

Tubular-supported catalytic membrane

The tubular supported catalytic membrane consists of a thin layer of Pd-impregnated, microporous γ-Al_2O_3 deposited on a tubular support made of macroporous α-Al_2O_3. The tubular supports used in this study were provided by Norton Company (Worcester, MA). The tubes had an average pore diameter of 6 μm, a wall thickness of 1.1 mm, and an external diameter of 4.9 mm. The properties of the two tubes used for this study are summarized in Table 1. They are referred to as tube nos. 2 and 3, respectively [following the numbering system of Cini (1991)].

The microporous, high surface area film was deposited on the inside of the tube using a sol-gel technique. The BET area of the tubular support and of the film were 1 and 130 m^2/g, respectively. The film loading for the two tubes were approximately 2% based on the α-Al_2O_3 tube mass. The details of the preparation and characterization of this type of catalytic support are described elsewhere (Cini et al., 1990).

The tubes were impregnated with Pd by an initial soaking for several hours in an aqueous solution of ammonium tetrachloropalladium (II) (initial concentration of 4.2×10^{-3} mol/L). The tubes were then dried at room temperature, calcined at 300°C for two hours in a flowing air stream, and then reduced in flowing hydrogen at 350°C for one hour. The Pd uptake determined by a UV spectrophotometric analysis of the salt solution amounted to approximately 2% of the dry γ-Al_2O_3 film mass (see Table 1). The 2 wt. % value is an upperbound value since some Pd is probably located in the α-Al_2O_3. The γ-Al_2O_3 film basis is used because at least 70% of the Pd is estimated to be located in the γ-Al_2O_3 film. This estimate is based on the film and support BET areas and the film loading (Table 1) and assumes that the Pd salt has the same affinity for the α- and γ-Al_2O_3. Moreover, the purposeful placement of the γ-Al_2O_3 film adjacent to the gas increases the likelihood that most of the reaction occurs there.

Surface-shell, catalytically-impregnated pellet

The 'pellet' used in the fully-wetted, single-pellet experiments consisted of a macroporous α-Al_2O_3 tube onto which a thin layer of microporous γ-Al_2O_3 was deposited. The tube was then impregnated with Pd. These two steps followed the same procedures used for the inside-wall-coated tubes described above. The core of the pellet support tube was filled with α-Al_2O_3 particles with normal size between 50 and 100 μm. For reasons discussed later, the 'pellet' was prepared to have essentially the same γ-Al_2O_3 film thickness and Pd loading as one of the tubes (no. 3). The γ-Al_2O_3 layer thickness was 50 μm for tube no. 3 and 55 μm for the "pellet" (no. 4 in Table 1). These measurements were made with a scanning electron microscope.

Experimental Setup and Procedures

Tubular-supported catalytic membrane experiment

The hydrogenation of α-methylstyrene (AMS) to cumene over a Pd/Al_2O_3 catalyst was selected as the model reaction. This particular system was chosen for several reasons. First,

Table 1. Properties of the Three Catalyst Samples Used in This Study

Sample No.	Sample Type	γ-Al_2O_3 Loading (wt. %) (γ-Al_2O_3 Basis)	Pd Loading (wt. %) (γ-Al_2O_3 Basis)	Length (cm)
2	Hollow Tube	2.11	2.5	12
3	Hollow Tube	1.99	1.82	12
4	Tube-Shaped Pellet	8.00	1.85	12

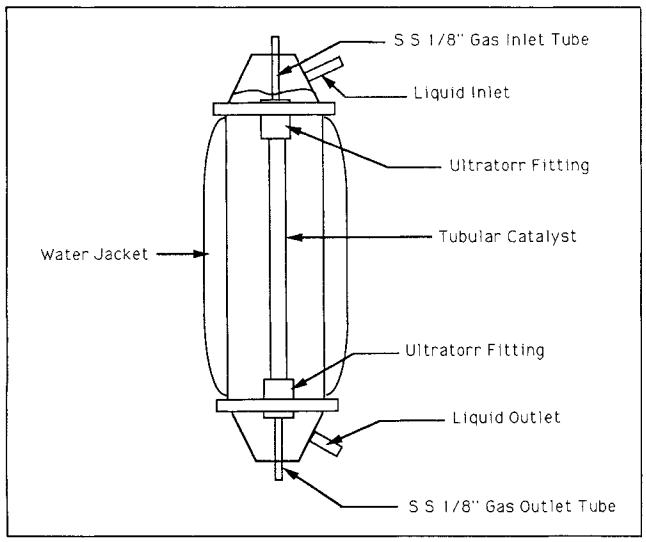

Figure 1. Tubular-supported catalytic membrane reactor used in the experimental study.

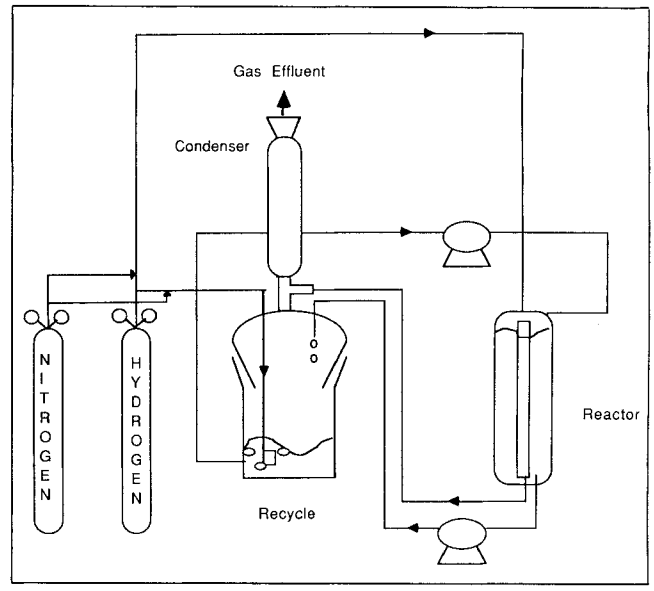

Figure 2. Tubular-supported catalytic membrane reactor experimental setup.

the reaction kinetics on Pd have been studied by others (e.g., Babcock et al., 1957; Satterfield et al., 1969; Turek et al., 1980; Nguyen, 1989; Funk et al., 1990). Second, cumene is the only measurable reaction product at low temperatures. Third, the reaction is mildly exothermic ($-\Delta H = 109$ kJ/mol), and the AMS and cumene are rather nonvolatile (normal boiling points are 165 and 152°C, respectively). Thus, nonisothermal effects (e.g., vaporization of liquid phase) are expected to be minimized. Fourth, the reaction is representative of a wide class of volatile-reactant-limited, metal-catalyzed, liquid-phase oxidations and hydrogenations.

The AMS (acquired from Kodak) had a purity of at least 98%. The polymerization inhibitor, *p*-tert-butylcatechol, was removed by soaking the AMS in γ-Al_2O_3 particles before use. In some experiments, the AMS was diluted with mesitylene (1, 3, 5-trimethylbenzene). The mesitylene (acquired from Kodak) had a purity of at least 98%. Both the nitrogen and hydrogen were Aero All Gas 'prepurified grade' with purities of at least 99.99 and 99.95 %, respectively. Drierite and molecular sieve traps were installed on the gas lines to remove traces of water and other impurities contained in the gas feed.

The reaction was carried out in a pyrex vessel containing a single tubular-supported catalytic membrane, as shown in Figure 1. The catalytic tube was connected to the inlet and outlet gas lines with Ultratorr fittings. The vessel was approximately 30-cm-long and has an inside diameter of 2.4 cm. An annular water jacket around the vessel provided control of the liquid-phase temperature. The gas and liquid flowed cocurrently downward.

A flowsheet of the experimental setup is shown in Figure 2. Since the conversion per pass to cumene was very low, the reactor was run in a semibatch mode. The AMS or AMS-mesitylene mixture was fed to the top of the reactor, pumped from the bottom of the reactor to the recycle unit, and eventually pumped back to the reactor. The residence time of the liquid phase in the reactor was typically about four minutes. For a typical volumetric flow rate of 25 cm^3/min used in our study, the liquid Reynolds numbers was 35, indicating laminar flow. Conversely, the gas was run continuously. After flowing through the core of the tube, it passed through a condenser to recover any vaporized organics and was then vented to the atmosphere. For a typical flow rate of 80 cm^3/min, the gas Reynolds number was about 5 indicating laminar flow as well. In some experiments, hydrogen was bubbled in the recycle unit to presaturate the liquid phase. In other experiments, nitrogen was used for stripping the hydrogen dissolved in AMS. In these two cases, the liquid phase is referred to as saturated and unsaturated liquid feed, respectively.

It was possible to heat the liquid phase up to 80°C whereas the gas phase could only be heated to 40°C. Most of the experiments were carried out at or below 40°C. Therefore, they were run isothermally. Heating cords powered by variable power supplies were wrapped around the gas and liquid lines and the reactor. The recycle unit was immersed in a water bath, the temperature of which was controlled by a hot plate. Three thermocouples were positioned in the liquid phase: one each in the effluent stream, in the feed stream, and at the bottom of the recycle unit. A fourth thermocouple was positioned in the gas-phase reactor inlet. One particular set of experiments described below required higher temperatures and could not be carried out under isothermal conditions: the temperature of the liquid phase exceeded that of the gas phase. Nevertheless, from the knowledge of gas- and liquid-bulk-phase temperatures, it was possible to estimate the temperature in the active region of the catalyst. These computed temperatures are referred to as "corrected temperatures." The details of the correction are given in the Appendix.

The overall reaction rate was determined by measuring the buildup of cumene in the liquid phase with a Hewlett Packard (model 5890) gas chromatograph. The chromatograph was operated in the splitless mode with a capillary column (J & W, Durobond Wax) and flame ionization detector. The reaction rate is described by the recycle-batch equation:

$$\text{Overall Reaction Rate} = \frac{V}{m}\left(\frac{dC_{\text{cum}}}{dt}\right) \tag{1}$$

where V is the average volume of liquid in the system over the time of the experiment, m is the mass of the tube (overall mass or active layer) and C_{cum} is the cumene concentration. For a typical run, six data points were collected one hour apart. To reach a pseudosteady state (dC_{cum}/dt = constant), the experiments were run for about one hour before starting sampling. Over a typical six-hour run, about 15 cm^3 of an initial 150 cm^3 of AMS was lost, of which 6 cm^3 was accounted for by sampling. The remainder was lost by vaporized liquid, not recovered by the condenser. We estimate that most of the vaporization occurred in the recycle unit, because the gas flow rate and the gas-liquid interfacial area were much higher there than in the inside of the tube. [See Cini (1991) for details.]

During the course of a typical experiment, it was observed that some liquid accompanied the effluent in the gas outlet line. The estimated flow rate of this "leak" was approximately 15-20 cm^3/h. The origin of the leak was either the Ultratorr fittings or from the tube wall itself. In either case, the existence of the leak implies that the inside wall was not completely "nonwetted." In the Analysis section, we rationalize that this leak did not have a significant impact on the reactor performance.

Fully-wetted, single-catalytic-pellet experiment

The reactor for the fully-wetted pellet experiments consisted of the single tube ("pellet") suspended in a glass vessel. The cylindrically-shaped glass reactor had an inner diameter of 3 cm and a total length of 35 cm. The reactor temperature was controlled by varying the circulating fluid (water or triethylene glycol) temperature in the jacket. A thermocouple was positioned halfway down the pellet and 6 to 7 mm from the surface.

The experimental setup was similar in design and operation to that of the tubular-supported membrane experiments. The liquid was fed to the top of the reactor where it ran down a thread from which the pellet was suspended, and than along the outside surface of the catalyst. Liquid that flowed off the pellet was pumped back to the recycle unit and eventually fed back to the reactor. The gas phase was run continuously and countercurrent to the liquid. Effluent gas flowed through a condenser before being vented. The liquid and gas flow rates were set to 21 and 75 cm^3/min, respectively, in all these experiments. The Reynolds number describing the thin-film flow was calculated to be approximately 160, which indicates that the liquid stream was laminar and rippled (Bird et al., 1960). (Indeed, ripples could be observed in the liquid film flowing down the pellet.) The average liquid film thickness was estimated to be 160 μm. The method used for estimating the overall reaction rate was the same as for the tubular-supported catalytic membrane experiments.

Results

Tubular-supported catalytic membrane reactor experiments were carried out over a range of different operating conditions. The five variables considered were the feed gas composition (hydrogen in nitrogen), the feed gas flow rate, the liquid composition (AMS in mesitylene), the degree of hydrogen saturation of liquid entering the reactor, and the catalyst temperature. In the fully-wetted, single-pellet experiments, two variables were examined: the pellet temperature and the degree of hydrogen saturation of liquid entering the reactor.

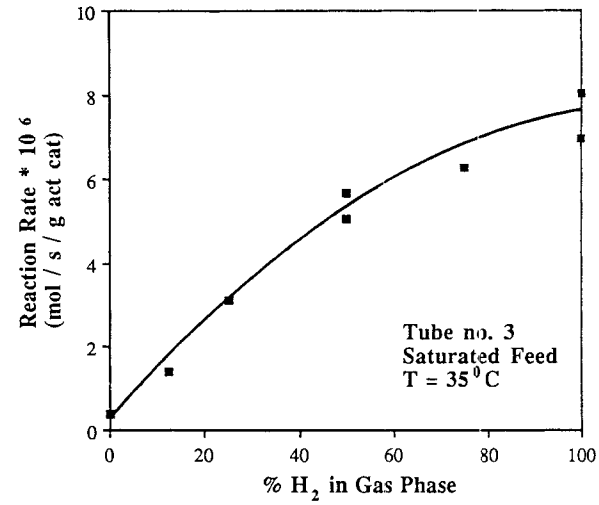

Figure 3. Dependence of the tubular reactor reaction rate on the partial pressure of hydrogen in the gas phase.

Experiments performed on tube no. 3 at 35°C with a hydrogen-saturated liquid feed.

The catalytic activity remained essentially constant over the course of a set of experiments with a particular tube. This was checked by reproducing the particular experiment that started the set at the end of a set of experiments. In every case, the results of repeated runs agreed to within ±15%.

Tubular-supported catalytic membrane reactor

Figure 3 shows the dependence of the overall rate on the volume fraction of hydrogen in the feed gas for tube no. 3. The total volumetric flow rate was maintained at 80 cm^3/min. The overall reaction rate is defined on a γ-Al_2O_3 film mass basis (for reasons discussed earlier). Pure hydrogen was bubbled in the recycle unit to presaturate the liquid before it entered the reactor. The rate monotonically increases with the volume fraction of hydrogen. The apparent order with respect to hydrogen is between 0.5 and 1. It should be noted that in the case of pure nitrogen gas feed, the only supply of hydrogen is from the presaturated liquid. Under these conditions, the overall rate is very low, about 5% of the rate obtained with a pure hydrogen gas.

Similar results were obtained with a nonsaturated AMS liquid feed (nitrogen used in bubbler). The data exhibited a fractional order dependence on the hydrogen volume fraction. [See Cini (1991) for details.]

Figure 4 shows the dependence of the overall rate on the gas flow rate obtained with tube no. 3 for a volume fraction of hydrogen of 0.1 and an unsaturated liquid feed. Within experimental error (noting that the rates are quite low), the rate levels off at higher flow rates, indicating minimal gas-side transport resistance.

Figure 5 shows the influence of the liquid-phase reactant composition (AMS in mesitylene) on the overall rate at 30°C for tube no. 2. Between 0 and 5 vol. % AMS, the rate increases rapidly. Above 10%, the rate is a weak function of the AMS concentration.

The impact of catalyst temperature is shown in Figures 6 and 7 in the form of apparent activation energy plots for tubes

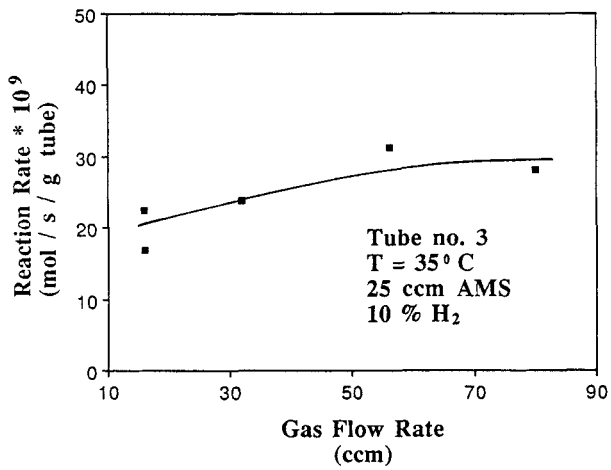

Figure 4. Dependence of the tubular reactor reaction rate on the gas flow rate.

Experiments performed on tube no. 3, at 35°C with a partial pressure of hydrogen of 0.1

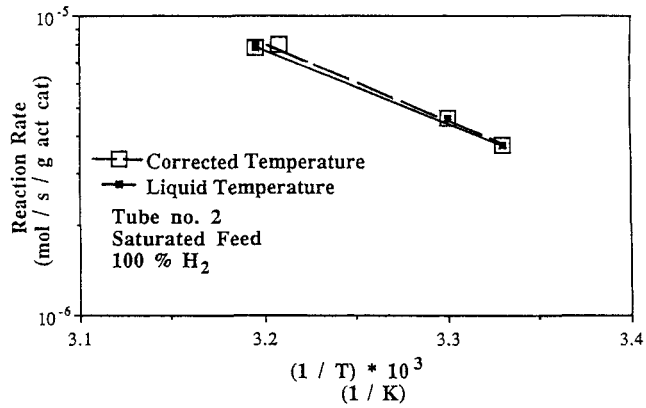

Figure 6. Dependence of the tubular reactor reaction rate on the temperature in the bulk liquid phase and on the estimated reactive zone temperature.

Experiments performed on tube no. 2 with a hydrogen-saturated liquid feed and a pure-hydrogen gas phase

nos. 2 and 3, respectively. As pointed out earlier, it was difficult to reliably heat the gas phase above 40°C. However, the liquid phase could be heated to 80°C. Thus, the temperature reported is that of the liquid; these are denoted by solid symbols. An estimate for the temperature of the active layer was computed for each run following the procedure in Appendix A. These corrected temperatures were used to replot the data; the open symbols are the data based on these corrections. Plots corresponding to the liquid temperature and corrected temperature data exhibit the same trends. Between 27 and 40°C (corrected temperatures), the dependence is linear (Figure 6). The slope corresponds to an apparent activation energy of approximately 43.5 kJ/mol. Above 45°C (Figure 7), there is a decrease in the slope. In this regime, the apparent activation energy is between 0 and 4 kJ/mol.

Fully-wetted, catalytically-shell-impregnated, single-pellet reactor

In this set of experiments, the outside surface of the surface-shell-impregnated "pellet" was wetted completely by a flowing liquid film. Experiments were carried out for both saturated and unsaturated feeds. Pure hydrogen was used as the gas, the flow rate of which was maintained at 75 cm^3/min. The liquid temperature was varied between 30 and 80°C. Hydrogen (nitrogen) was bubbled in the recycle unit to presaturate (strip) the liquid with (of) hydrogen before entering the reactor.

Figure 8 shows that the saturated and nonsaturated rate data exhibit a nearly linear dependence on reciprocal temperature. For reasons discussed below, the reported rate is on a γ-Al_2O_3 film volume basis. For comparison, Figure 8 provides the rate data obtained with tube no. 3. For the entire temperature range

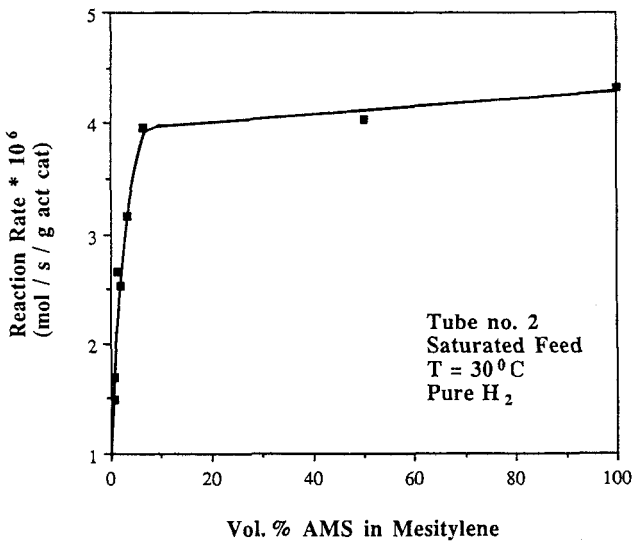

Figure 5. Dependence of the tubular reactor reaction rate on the vol. % of AMS in mesitylene.

Experiments performed on tube no. 2, at 30°C with a hydrogen-saturated liquid feed and a pure-hydrogen gas phase

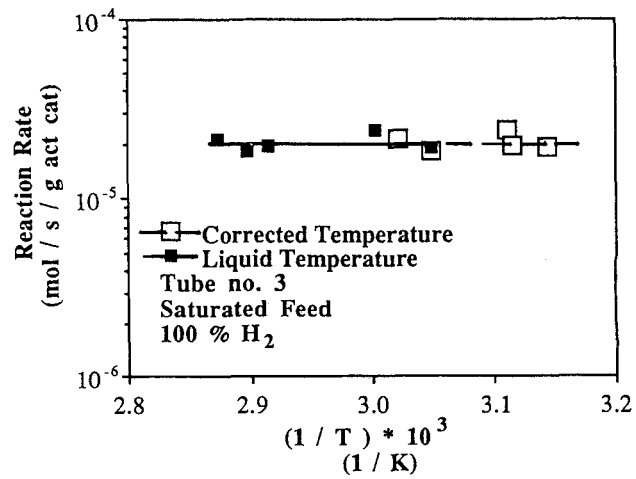

Figure 7. Dependence of the tubular reactor reaction rate on the temperature in the bulk liquid phase and on the estimated reactive zone temperature.

Experiments performed on tube no. 3, with a hydrogen-saturated liquid feed, and a pure-hydrogen gas phase.

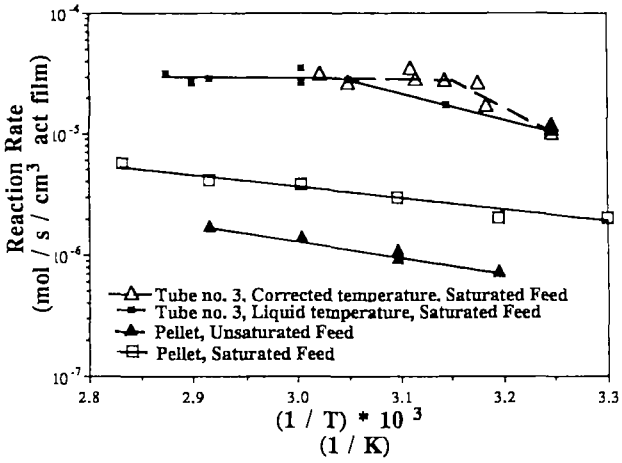

Figure 8. Dependence of the single pellet reactor reaction rate on the reaction temperature.

Experiments performed on tube no. 4, using a pure-hydrogen gas phase. Both saturated and nonsaturated AMS liquid feed are shown. For comparison, the rate data for the hollow tube catalyst (no. 3) is shown.

the hollow tube rates exceeds the rate observed with the fully-wetted "pellet."

Analysis and Discussion

In this section, our objectives are threefold. First, the transport-reaction interactions occurring in the tubular-supported catalytic membrane and fully-wetted pellet are elucidated. The pertinent questions to be addressed are which of the reactants is limiting and which of the processes controls the rate. This analysis helps to determine the type of multiphase reactions, for which the tubular-supported membrane reactor is best suited and the window of operating conditions (reaction temperature, gas and liquid flow rates, and degree of saturation of the liquid phase by the volatile reactant), for which the rate is maximized. Our second objective is to propose potential rate expressions that predict the intrinsic reaction kinetics of AMS hydrogenation. This step is possible if transport limitations indeed are estimated to be negligible under some conditions. Third, the hollow-tube catalyst performance is assessed in light of the performance of the fully-wetted "pellet."

Limiting reactants

The low solubility of hydrogen compared to the bulk AMS concentration makes it the limiting reactant under most conditions. For example, at 40°C the solubility of hydrogen in AMS in 3.1×10^{-6} mol/cm^3, whereas the molar concentration of AMS is 7.5×10^{-3} mol/cm^3 (Funk et al., 1991). A key point is that most of the hydrogen consumed comes directly from the gas (Figure 3). Indeed, this was the original intent in the catalyst design. For a gas devoid of hydrogen, the only supply of hydrogen comes from the feed liquid that is presaturated with hydrogen. The results in Figure 3 demonstrate that the rate is very low under such conditions. Conversely, when the feed gas is pure hydrogen, the rate is about a factor of 20 higher than the rate obtained in the absence of hydrogen in the feed gas. These results confirm the intuitive expectation that direct transport from the gas is more efficient. Such is the case for the effectiveness enhancement phenomena observed with the partially-wetted pellet (Harold and Ng, 1987; Funk et al., 1991).

If the AMS feed concentration is lowered significantly, there is a measurable impact of the AMS concentration. Figure 5 shows that above 10 vol.% AMS (in mesitylene), the rate is essentially zeroth order with respect to AMS. Below 5 vol. %, the rate is almost linear with respect to AMS. At sufficiently high catalyst temperature, depletion of AMS that is in excess in the bulk may occur within the catalytic membrane. This point is examined below.

Rate-controlling processes

There are six possible rate-controlling processes that may explain the various trends in the data. The first five assume that the active film is completely filled with liquid, and therefore only a liquid-phase catalytic reaction occurs. The sixth possibility relaxes this assumption, as discussed below.

The first two processes involve hydrogen transport: (1) diffusion within the Pd impregnated γ-Al_2O_3 film, and (2) transport through the liquid film covering the inside wall of the tube. Regarding (2), recall that some liquid appeared in the gas effluent, suggesting that the inside tube wall may have been wetted by a thin liquid film. Potential limitations, due to the transport of hydrogen in the α-Al_2O_3 support, can be ruled out, because the hydrogen that reacts is supplied almost solely from the gas side. Moreover, gas-side hydrogen transport limitations are unlikely based on the measured impact of the gas flow rate (Figure 4). Gas-side hydrogen limitations are unlikely especially for hydrogen fractions exceeding 0.5.

The third and fourth possible rate-controlling processes are intraparticle diffusion of AMS in the γ-Al_2O_3 film and the α-Al_2O_3 tube, respectively. Under conditions of a high rate, depletion of AMS could occur within the active film positioned adjacent to the rapidly supplied hydrogen, simply because of the longer diffusion path traversed by the nonvolatile reactant. The position of this "reaction plane" would be determined by the relative supply rates of AMS and hydrogen from opposite sides of the membrane. The external transport of AMS from the bulk liquid phase is not likely to be rate-limiting, because in most of the experiments the liquid was essentially pure AMS: the amount of cumene produced during a run was typically less than 2 wt. %. This, however, does not mean that the local intraparticle cumene concentration is also negligible compared to the AMS concentration; thus, AMS pore diffusion limitations are possible.

The fifth possible controlling process is an intrinsic reaction process. Indeed, we show below that the tubular catalyst operates with negligible transport resistance under some conditions.

The sixth possibility acknowledges that some pore emptying of the active film may have occurred because of the reaction heat effects. Harold (1988) has shown that a catalyst that is wetted on one side and nonwetted on the other, and catalyzes an exothermic reaction, may not be completely filled by the imbibing liquid. The combination of an exothermic reaction heat, a volatile liquid phase, and ineffective heat removal by the gas increase the likelihood of pore emptying and a resultant gas-phase catalytic reaction. Under such conditions, transport within the gas-filled pores would likely be the slowest processes.

Our approach of eliminating some of the six processes as rate-controlling for a given set of conditions is based on an apparent activation energy analysis. The success of this analysis relies on knowledge of the intrinsic activation energy which was measured by standard means in a few other studies. The first step is to derive the expressions for the apparent activation energy for the first four cases identified above. (The fifth and sixth cases are treated separately below.)

The first four cases can be classified as either hydrogen-limiting or AMS-limiting. To simplifying the analysis, the rate is assumed to be first order with respect to the limiting reactant and zeroth order with respect to the reactant in excess. The shell-impregnated tubular catalyst is approximated by a slab made of two layers: one very thin which is catalytically active and the other considerably thicker which is catalytically inert. Note that hydrogen penetrates the tube from the bulk gas-side, whereas AMS penetrates from the bulk liquid side, diffusing first through the inert layer before reaching the active layer. Despite these differences, both the hydrogen-limited and AMS-limited situations can be treated in a similar manner.

The active layer effectiveness (η_a) is defined as the ratio of the overall reaction rate to the rate that would be observed in the absence of any intraparticle or external mass transport limitations. It can be expressed as:

$$\frac{1}{\eta_i} = \frac{\phi_i}{\tanh\phi_i} + \frac{\phi_i^2}{Sh_i} \tag{2}$$

where ϕ_i and Sh_i are defined differently for each case (i denotes the limiting reactant H_2 or AMS). The overall rate satisfies

$$\text{Rate} = kC_{H_2}C_{AMS}\eta_i \tag{3}$$

When hydrogen is the limiting reactant, ϕ_{H_2} and Sh_{H_2} are equal to:

$$\phi_{H_2} = \delta_a\sqrt{\frac{k'}{D_{eH_2}}} \tag{4}$$

$$Sh_{H_2} = \frac{k_{H_2}\delta_a}{D_{eH_2}} \tag{5}$$

respectively, where δ_a is the active layer thickness, D_{eH_2} is the effective diffusion coefficient of hydrogen in the liquid-filled (AMS and cumene) intraparticle region of the tube and k_{H_2} is an overall mass transfer coefficient describing the hydrogen transport through a thin liquid film on the inside tube wall. The pseudo first-order rate constant k' is equal to kC_{AMS}.

When AMS is the limiting reactant, ϕ_{AMS} is given by:

$$\phi_{AMS} = \delta_a\sqrt{\frac{k''}{D_{eAMS}}} \tag{6}$$

where D_{eAMS} is the effective diffusion coefficient of AMS in the liquid-filled inert intraparticle layer. The pseudo first-order rate constant k'' is equal to kC_{H_2}. Sh_{AMS} describes the transport of AMS from the bulk liquid to the active layer support interface. Its expression is given later in the analysis.

Expressions for the apparent (or observed) activation energy, E_{obs}, are derived using the definition

$$E_{obs} = -R\frac{d(\ln \text{Rate})}{d(1/T)} \tag{7}$$

The four transport-limited cases are now analyzed.

Case 1: Hydrogen Transport in Active Region. In this case, ϕ_{H_2} and Sh_{H_2} are both large, and Eqs. 2 and 3 give:

$$\text{Rate} = \frac{kC_{AMS}C_{H_2}}{\phi_{H_2}} = \frac{C_{H_2}(C_{AMS}kD_{eH_2})^{0.5}}{\delta_a} \tag{8}$$

Thus,

$$E_{obs} = E_{sat} + \frac{E_{in} + E_{dH_2}}{2} \tag{9}$$

where E_{sat}, E_{in}, and E_{dH_2} are the activation energies describing the temperature dependence of the hydrogen solubility (C_{H_2}), the intrinsic kinetics (k), and the hydrogen diffusivity (De_{H_2}), respectively.

Case 2: Hydrogen Transport through Thin Liquid Film. In this case, the second term on the right hand side of Eq. 2 dominates and the rate (Eq. 3) is approximated by:

$$\text{Rate} = kC_{AMS}C_{H_2}\frac{Sh_{H_2}}{\phi_{H_2}^2} \tag{10}$$

or

$$\text{Rate} = \frac{C_{H_2}Sh_{H_2}D_{eH_2}}{\delta_a^2} \tag{11}$$

The flow of the liquid film inside the tube wall is considered laminar. Using the mass transfer correlation for laminar flow along a flat plate (Cussler, 1984) SH_{H_2} can be expressed as:

$$Sh_{H_2} = FD_{H_2}^{-1/3}\mu_{AMS}^{-1/6} \tag{12}$$

where F is a function that includes all the variables that do not vary appreciably with temperature, and μ_{AMS} is the viscosity of AMS. The rate is approximated by:

$$\text{Rate} = \frac{FC_{H_2}D_{eH_2}}{\delta_a^2 D_{H_2}^{1/3}\mu_{AMS}^{1/6}} \tag{13}$$

Assuming that

$$D_{eH_2} = \frac{\epsilon}{\tau}D_{H_2} \tag{14}$$

where ϵ and τ are the void fraction and the tortuosity of the support, respectively, the rate can be rewritten as:

$$\text{Rate} = \frac{F\epsilon^{1/3}C_{H_2}D_{eH_2}^{2/3}}{\tau^{1/3}\delta_a^2\mu_{AMS}^{1/6}} \tag{15}$$

Thus, the observed activation energy is equal to (using Eq. 7):

$$E_{obs} = E_{sat} + \frac{2}{3} E_{d\mathrm{H}_2} - \frac{1}{6} E_{\mu_{AMS}} \tag{16}$$

where $E_{\mu AMS}$ is the apparent activation energy describing the temperature dependence of the liquid viscosity.

Case 3: AMS Transport in Active Region. In this case, ϕ_{AMS} and Sh_{AMS} are large, and Eqs. 2 and 3 give:

$$\text{Rate} = \frac{kC_{AMS}C_{\mathrm{H}_2}}{\phi_{AMS}} = \frac{C_{AMS}\sqrt{kD_{eAMS}C_{\mathrm{H}_2}}}{\delta_a} \tag{17}$$

Thus, the apparent activation energy is given by:

$$E_{obs} = \frac{E_{in} + E_{sat} + E_{dAMS}}{2} \tag{18}$$

Case 4: AMS Transport in Inert Region. In this case, it is possible to lump the intraparticle transport of AMS in the inert zone and the external transport into one resistance by defining an overall mass transfer coefficient, k^o_{AMS}:

$$\frac{1}{k^o_{AMS}} = \frac{1}{k_{na,AMS}} + \frac{1}{k_{l,AMS}} \tag{19}$$

where $k_{na,AMS}$, and $k_{l,AMS}$ are the mass transport coefficients describing the transport of hydrogen in the inert intraparticle layer and the liquid bulk, respectively. The former is approximated by the ratio $D_{e\mathrm{H}_2}/\delta_{na}$. Using Eqs. 2 and 3, the overall rate is approximated by:

$$\text{Rate} = \frac{kC_{AMS}C_{\mathrm{H}_2}Sh_{AMS}}{\phi^2_{AMS}} \tag{20}$$

where

$$Sh_{AMS} = \frac{k^o_{AMS}\delta_a}{D_{eAMS}} \tag{21}$$

In the limiting (and more likely) case in which the intraparticle resistance is significantly larger than that in the liquid bulk ($k_{l,AMS} \gg k_{na,AMS}$) Eq. 19 predicts that $k^o_{AMS} \sim k_{na,AMS}$, and thus $Sh_{AMS} = \delta_a/\delta_{na}$. Using this result and Eqs. 6, 20 and 21, we get:

$$\text{Rate} = \frac{C_{AMS}k^o_{AMS}}{\delta_a} \tag{22}$$

In this case, we get

$$E_{obs} = E_{dAMS} \tag{23}$$

The mathematical expressions for the observed activation energies obtained for cases 1-4 described above are compiled in Table 2. Numerical estimates for E_{obs} are also provided and are based on estimated values for E_{sat}, $E_{\mu AMS}$, and $E_{d\mathrm{H}_2}$. These were obtained as follows. Ma (1966) measured $E_{d\mathrm{H}_2}$ and found it equal to 12.6 kJ/mol. E_{sat} was determined by Herskowitz et al. 1978 to be equal to approximately 4.2 kJ/mol. For determining $E_{\mu AMS}$, we used viscosity-temperature data obtained for metaxylene that has a structure similar to that of AMS. For estimating E_{dAMS}, we used the Stokes-Einstein model for D_{dAMS}. These approximations lead to values of -9.2 and 10.9 kJ/mol for $E_{\mu AMS}$ and E_{dAMS}, respectively. Several investigators carried out AMS hydrogenation to cumene on supported Pd for conditions similar to our study. The activation energies measured in these different cases are compiled in Table 3. They vary from 19.7 to 38.1 kJ/mol. This rather wide range seems to indicate that for the lower measured activation energies, the reaction rate was not controlled by the kinetics but rather by the transport of the reactants. The more recent data seem to agree on the value of approximately 37-38 kJ/mol for the intrinsic activation energy.

Case 5: Intrinsic Liquid-Phase Catalytic Reaction Kinetics. This case is treated differently since by definition transport limitations are insignificant ($\eta = 1$). As shown in Table 2, the apparent activation energy is equal to its intrinsic value, $E_{obs} = E_{in}$.

Case 6: Transport in Gas-Filled Pores. This final case is the most difficult one to handle because of the many processes that occur simultaneously in a partially-filled pellet. Even in the simplest scenario, a single distinct gas-liquid interface is positioned within the active layer (following Harold, 1988). Reaction and transport in both gas- and liquid-filled pores occur. Some of the evolved heat is used to vaporize the convecting liquid. Our recent simulations of a bimolecular reaction reveal that severe concentration gradients can exist in both regions of the pellet (Watson and Harold, 1990). The rate depends on the composition of the gas within the pores, which in turn depends on the temperature and the volatilities of the liquid components. Thus, it is difficult to predict the expected apparent activation energy without specific calculations for AMS hydrogenation. The very low apparent activation energy at higher temperatures might indicate a transport-controlled, gas-phase catalytic reaction.

Now that the apparent activation energies for the first five cases have been estimated, the data can be analyzed. Recall

Table 2. Estimated Apparent Activation Energies for Five Rate-Controlling Situations

Case 1	Case 2	Case 3	Case 4	Case 5
Transport of H_2 in Active Porous Region	Transport of H_2 in Liquid Film on Gas Side	Transport of AMS Active Porous Region	Transport of AMS in Nonactive Porous Region	Intrinsic kinetics
$\frac{E_{in} + E_{d\mathrm{H}_2}}{2} + E_{sat}$	$\frac{2}{3} E_{d\mathrm{H}_2} + E_{sat} - \frac{1}{6} E_{\mu_{AMS}}$	$\frac{E_{in} + E_{sat} + E_{dAMS}}{2}$	E_{dAMS}	E_{in}
32.2 kJ/mol	13.8 kJ/mol	29.3 kJ/mol	10.9 kJ/mol	43.5 kJ/mol

Table 3. Measured Activation Energies for AMS Hydrogenation on Different Pd Catalysts

Authors	Pres. atm	T °C	Support	Particle Dia μm	Reactor Type	E kJ/mol
Babcock et al. (1953)	2	24–57	0.5 wt. % Pd on Alumina	3180	Trickle Bed	19.7
Satterfield et al. (1969)	1	70	0.5 wt. % Pd on Alumina	50	String of Pellets	31.8
Turek et al. (1980)	1–15	15–50	Pd on Alumina	20–100	Stirred Autoclave	38.9
Mai-Thanh (1989)	1–3	30–40	5 wt. % Pd on carbon	<50	Stirred Autoclave	38.1
Cini et al. (1990)	1	27–40	2 wt. % Pd on Alumina	50	Tubular Reactor	43.5

that the apparent activation energy for tube no. 3 had two different values depending on the temperature range (Figures 6 and 7). Between 27 and 40°C, the apparent activation energy is estimated to be 43.5 kJ/mol. Between 45 and 58°C, the apparent activation energy is 0–4 kJ/mol.

Below 40°C, the close agreement of the apparent activation energy with data from previous AMS kinetics studies (Table 3) suggests that the rate is kinetically controlled. Comparison of the measured activation energy between 45 and 58°C with the predicted values in Table 2 reveals that cases 2 and 4 give the closest agreement. In addition, case 5 cannot be ruled out because of a possible kinetic shift in the apparent activation energy (the studies referenced in Table 3 did not provide kinetics data above 45°C). We can rule out case 2 based on the following arguments. As shown below in the analysis of the fully-wetted single-"pellet" data, the overall rate is controlled by the transport of hydrogen in the active intraparticle region of 50-μm thickness. That is, the liquid film flowing over the pellet, which is estimated to be 160-μm-thick, does not pose a significant resistance to the transport of hydrogen from the gas phase to the surface of the catalyst. Given that the potential liquid film covering the tube inside wall is estimated to be about three times thinner than the film flowing over the pellet, [based on the measured leak rate; see Cini (1991) for details], we conclude that it does not pose a significant resistance to the transport of the volatile reactant. Thus, the remaining possibilities are case 4 (AMS pore diffusion in inert support), case 5 (liquid-phase reaction kinetics), and case 6 (gas-phase catalytic reaction).

This analysis at least is overall kinetics evidence that the tubular-supported membrane catalyst operates with negligible mass transport limitations below 40°C. Only for lower hydrogen partial pressures and flow rates, does the gas-side resistance become important in this temperature range. Above 45°C, AMS transport limitations may appear. Thus, the tubular design is a good one for effectively supplying the usually limiting volatile reactant. Moreover, these findings suggest that it may be possible to switch from a regime in which the reaction is volatile reactant limited to one in which the nonvolatile reactant supply controls the rate. Quite possibly, the regime of kinetics control can be extended by reducing the wall thickness of the α-Al_2O_3 tube.

Kinetics

The last section demonstrated that the tubular-supported catalyst can operate without transport limitations at lower temperatures. This invites the possibility of exploiting the data for intrinsic kinetics analysis of multiphase reactions. The objectives of this section are to compare the kinetics trends observed in previous studies and the current study for Pd-catalyzed AMS hydrogenation.

Previous studies have shown that the reaction rate is an increasing function of the hydrogen concentration. Turek et al. (1980) reported a rate which is first order with respect to hydrogen. Babcock et al. (1957) observed a reaction order with respect to hydrogen of between 0 and 1. In our case, the measured reaction order is between 0.5 and 1. The dependence on AMS is more complex. We observed that the rate increases very sharply with AMS concentration, when the AMS is sufficiently dilute (below 10 vol. %). For sufficiently high AMS concentration, the rate is independent of AMS. These findings agree with Turek et al. (1980). Babcock et al. (1957) reported a slight maximum in the dependence of the rate on AMS concentration.

A few kinetic models have been proposed to predict these trends. An Eley-Rideal (ER)-type rate expression was proposed by Turek et al. (1980):

$$r=\frac{A\,P_{H_2}C_{AMS}}{1+B\,C_{AMS}} \tag{24}$$

Rate equation (Eq. 24) predicts the AMS-apparent order shifts from unity to zero, as the AMS concentration is increased. It also predicts a first-order dependence on hydrogen. The latter prediction does not agree with our observations or those of Babcock et al. (1957). Moreover, the model cannot predict a negative order rate dependence on AMS observed by Babcock et al. (1957).

A Horiuti-Polanyi mechanism (HP) has been proposed for other noble-metal-catalyzed, liquid-phase hydrogenation reactions (e.g., cyclohexene hydrogenation on Pt, Madon et al., 1978). The HP mechanism consists of the following steps:

1. $H_2+2X_1<=>2HX_1$
2. $AMS+X_2<=>AMSX_2$
3. $AMSX_2+HX_1<=>AMSX_2H$
4. $AMSX_2H+HX_1 => \text{Cumene} + X_1+X_2$

Rate expressions derived from the mechanism in the absence and presence of competitive adsorption respectively, are:

$$r=\frac{A\sqrt{P_{H_2}}C_{AMS}}{(1+B\sqrt{P_{H_2}})\,(1+CC_{AMS})} \tag{25}$$

Table 4. Apparent Turnover Numbers (Ω) for the Hollow Tube (this study) vs. a String of Spherical Pellets

Temp. °C	40	50
Tube Rate × 10^7 (mol/s/g cat)	2.36	4.84
Pellet Rate × 10^7 (mol/s/g cat)	0.86	1.13
$\Omega_{Tube} \times 10^2$ (s^{-1})	6.9	14.1
$\Omega_{Pellet} \times 10^4$ (s^{-1})	9.2	12.0
$\Omega_{Tube}/\Omega_{Pellet}$	75	117

Satterfield et al. (1969)

$$r = \frac{A\sqrt{P_{H_2}}C_{AMS}}{(1 + B\sqrt{P_{H_2}} + CC_{AMS})^2} \tag{26}$$

where A, B, and C are kinetic parameters.

Both HP models can predict most of the trends in our data (Figures 3 and 5). However, the HP mechanism with noncompetitive adsorption (Eq. 25) fails to predict the negative-order dependence on AMS observed by Babcock et al. (1957) and the first-order dependence on hydrogen observed by Turek et al. (1980). On the other hand, the HP mechanism with competitive adsorption (Eq. 26) can predict the negative-order dependence on AMS. However, it is still incompatible with a first-order dependence on hydrogen.

Clearly, a more detailed experimental study is needed for further discrimination. A main point we would like to underscore is that the tubular supported membrane reactor has the capability to carry out kinetic analyses of multiphase reactions.

Performance Comparisons

Comparison to a string of fully-wetted pellets (Satterfield et al., 1969)

A revealing means of comparing the performance of the tubular-supported catalytic membrane reactor to the more conventional trickle-bed reactor is to compute catalyst utilization or effectiveness. This was the approach we used in a previous modeling study (Harold et al., 1989). Another way is to compare apparent turnover numbers. The turnover number is defined as the frequency with which reaction occurs on a catalytic site. It is a precise measure of the intrinsic catalytic activity and utilization. In this section, we compare turnover number estimated for the catalytic membrane and for a string of fully-wetted catalytic pellets.

Satterfield et al. (1969) carried out the hydrogenation of AMS to cumene on a string of Pd shell-impregnated γ-Al_2O_3 pellets (0.825 cm dia., 1 wt. % Pd), which could be considered as a prototype trickle-bed reactor. The reaction, catalyst, and operating conditions are quite similar to those of our catalytic tube experiments.

The three key differences between the tubular catalyst (tube no. 3; see Table 1) and the pellets are the overall Pd loading (2 vs. 1 wt. %), the active layer thickness (50 μm vs. 2,000 μm), and the degree of Pd impregnation uniformity in the surface shell (nonuniform for pellets). Regarding the latter point, the Pd was distributed nonuniformly. It was essentially uniform over the first 100 μm and then dropped steadily, increasing back to its surface concentration in a band located 1,750 to 2,000 μm in from the outside surface, and then decreasing rapidly to zero. Hence, the intraparticle diffusion limitations are expected to be more severe for the pellets than for the tube.

Despite differences in the Pd loading, a comparison is revealing. Table 4 summarizes the results of estimated turnover numbers (denoted Ω) for tube no. 3 and for the string of pellets at two temperatures (40 and 50°C). The calculations assume that the Pd deposited on the supports is completely accessible for reaction in both systems (100% dispersion). The results reveal that the turnover numbers obtained with the tube are significantly larger than those obtained with the string of pellets. In fact, the tube turnover numbers exceed the pellet turnover numbers by almost a factor of 100. In addition, the widening gap between the overall rates obtained with the two catalysts with increasing temperature suggests that the higher the activity, the better the catalytic tube performs compared to the fully-wetted pellets.

Comparison to the fully-wetted single tubular pellet

The purpose of the fully-wetted single tubular pellet experiment was to measure as directly as possible the benefit gained from the partial wetting achieved with the hollow tube design. To isolate the partial wetting effect, it is necessary for the hollow tube and the fully-wetted pellet to have the same degree of intraparticle diffusion limitations or, equivalently, the same active region diffusion lengths. Since the active layers of both catalysts can be approximated by slabs that are penetrated by the limiting reactant hydrogen from one side only, their diffusion lengths are equal to the actual thickness of the active layers. This approximation is valid because: (1) the active layers of both catalysts are very thin compared to their respective inert regions; and (2) even though the hydrogen can penetrate from both the gas and liquid sides of the hollow tubular catalyst, it was shown earlier that virtually all the hydrogen that reacts comes from the gas side. This confirms previous model predictions of Harold et al. (1989).

Tube no. 3 was used for the comparison with the fully-wetted tubular "pellet." The active layer thickness for the catalytic tube and of the "pellet" were virtually equal: 50 vs. 55 μm. For the comparison to be as meaningful as possible, other features such as the operating conditions, the catalyst morphologies, and their activities were made as similar as possible. Despite the precautions taken for preparing virtually "identical" catalysts, one difference could not be avoided. It was determined that more of the γ-Al_2O_3 deposited on the tubular pellet penetrated the α-Al_2O_3 pores. That is, a higher loading of γ-Al_2O_3 was required to give approximately the same γ-Al_2O_3 film thickness (8 wt. % vs. 2 wt. %). However, we note that the presence of Pd-impregnated γ-Al_2O_3 located within the macropores should not contribute significantly to the rate, because for the conditions employed intraparticle hydrogen concentration gradients are likely to be so large that most of the hydrogen reacts within the external Pd-impregnated film.

First, we shall discuss the tubular pellet performance data. Figure 8 reveals an apparent activation energy of approximately 21-25 kJ/mol. This value can be compared to the predicted apparent activation energies of cases 1, 2 and 3 in Table 2 (case 4 is inapplicable). Case 3 (rate-controlled by the trans-

port of AMS in the active intraparticle region) can be ruled out for the following reason. It was shown earlier that between 27 and 40°C, the tubular reactor operated in the intrinsic kinetic regime. With the "pellet design," the Pd is even more accessible to the AMS because the nonvolatile reactant does not have to diffuse through an inert intraparticle region. Thus, between 27 and 40°C, the intraparticle transport of AMS, which is in large excess, is an unlikely rate-controlling process. The fact that the observed activation energy is slightly less than the predicted case 1 value (see Table 2) may suggest some rate limitation due to the external supply of hydrogen. Recall that for similar conditions (27–40°C), the hollow tube catalyst suffered no transport limitations.

For the comparison, the overall rate is expressed on a volume of active layer basis. This basis is better suited for comparing the performances of the two catalyst types, because we believe that most of the reaction occurs in the thin layer. Figure 8 shows that for a hydrogen presaturated liquid feed, the reaction rate for the tubular membrane is five to seven times that for the fully-wetted single pellet. This difference in performance is a direct measure of the benefit gained with partial wetting in a volatile-reactant-limited multiphase system. We showed earlier that the performance of the catalytic tube does not depend on the degree of saturation of the liquid phase with hydrogen, since most of the hydrogen supplied to the reactive region comes directly from the gas. Conversely, the performance of a fully-wetted pellet depends strongly on the degree of saturation of the liquid phase with hydrogen, since the gas doe not contact the pellet surface directly (Figure 8). The hollow tube rate is 15 to 20 times better than the pellet exposed to the unsaturated liquid. Given the similarity in catalyst properties and operating conditions, we conclude that the improved performance is a direct result of the partial wetting of the catalyst achieved with the hollow-tube design.

Concluding Remarks

In this study, we have developed the tubular supported catalytic membrane as a new type of multiphase catalyst. Its design permits a segregation of the gas and liquid phases, thus allowing the external transport of the limiting volatile reactant to the surface of the catalyst. We have demonstrated that the prototype single-tube reactor performs quite well without any major operational difficulties.

The partial wetting feature and the thin active film have been shown to combine to provide exceptional efficiency in the supply of the volatile reactant for a model of olefin hydrogenation. Indeed, the hydrogen predissolved in the liquid feed contributes little to the reaction, unlike its strong contribution in the fully-wetted trickle-bed reactor. For temperatures below 40°C, the rate essentially is kinetically-controlled and the catalyst utilization is nearly complete. Our analyses suggest that possible transport limitations in the supply of the nonvolatile reactant may occur at higher temperatures. Also, nonisothermal effects cannot be ruled out. Most significantly, the benefit gained from the partial wetting of the tubular-supported catalytic membrane was quantified by directly comparing its overall rate to that of the fully-wetted, surface-shell-impregnated pellet, considered to be the prototype trickle-bed. The partial wetting was shown to increase the rate by up to a factor of 20.

These findings indicate that if a multiphase catalytic reaction is likely to be severely volatile-reactant-limited, then the hollow catalytic tube reactor may be the reactor of choice. Clearly, other factors must be taken into account to make this decision, such as throughput, pressure drop, reliability, and safety. Catalyst utilization improvements may not be sufficient to overcome drawbacks in these other factors. However, improvements in desired product selectivity may be sufficient.

Acknowledgment

This research was supported by the ACS Petroleum Research Fund, grant no. 21189-AC7.

Notation

A = volatile reactant or kinetic constant
B = nonvolatile reactant or kinetic constant
C = concentration or kinetic constant
C_{AMS} = concentration of AMS in the bulk liquid phase
C_{cum} = cumene concentration
C_{H_2} = concentration of dissolved hydrogen in the bulk liquid phase
D_{eAMS} = effective diffusion coefficient of AMS
D_{eH_2} = effective diffusion coefficient of hydrogen in AMS
D_{H_2} = diffusion coefficient of hydrogen in AMS
E_{dH_2} = $-R\,[d(\ln D_{eH_2})/d(1/T)]$
E_{in} = intrinsic activation energy
E_{obs} = $-R\,[d(\ln \text{Rate})/d(1/T)$
E_{sat} = $-R\,[d(\ln C_{H_2})/d(1/T)]$
$E_{\mu_{AMS}}$ = $-R[d(\ln \mu_{AMS})/d(1/T)]$
F = function that appears in Eq. 12
h = heat transfer coefficient (Appendix)
k = second-order rate constant
k' = kC_{AMS}
k'' = kC_{H_2}
k^o_{AMS} = overall mass transfer coefficient for AMS (Eq. 19)
k_{H_2} = overall mass transfer coefficient for hydrogen (Eq. 5)
$k_{l,AMS}$ = mass transfer coefficient for AMS in liquid bulk
$k_{m,AMS}$ = mass transfer coefficient for AMS in inert region
L = tube length
m = mass of active catalyst
P_{H_2} = partial pressure of hydrogen
R = Universal gas constant
r = intrinsic rate
S = exchange surface area (Appendix)
t = time
T = temperature
V = average volume of liquid in reactor setup during experiment

Greek letters

δ_a = active layer thickness
δ_{na} = thickness of (nonactive) support layer
ϵ = void fraction
η = catalyst effectiveness
μ_{AMS} = viscosity of AMS
λ = thermal conductivity
ϕ_a = $\delta_a \sqrt{k/D_e}$
ϕ_{AMS} = $\delta_a \sqrt{k''/D_{eAMS}}$
ϕ_{H_2} = $\delta_a \sqrt{k'/D_{eH_2}}$
Φ = heat flux (Appendix)
τ = tortuosity

Literature Cited

Babcock, B. D., G. T. Mejdell, and O. A. Hougen, "Catalyzed Gas-Liquid Reactions in Trickle-Bed Reactors," *AIChE J.*, **15**, 229 (1957).
Bird, R. B., W. E. Stewart, and E. N. Lightfoot, *Transport Phenomena*, 406 (1960).

Cini, P., PhD Dissertation, University of Massachusetts, Amherst (1991).
Cini, P., S. R. Blaha, M. P. Harold, and K. Venkataraman, "Preparation and Characterization of Modified Tubular Ceramic Membranes for Use as Catalyst Supports," *J. of Memb. Sci.*, **55**, 199 (1991).
Cussler, E. L., *Diffusion: Mass Transfer in Fluid Systems*, 295, Cambridge, London (1984).
de Vos, R., V. Hatziantoniou, and N. H. Schoon, "The Cross-Flow Catalyst Reactor. An Alternative for Liquid-Phase Hydrogenations," *Chem. Eng. Sci.*, **37**, 1719 (1982).
Funk, G. A., M. P. Harold, and K. M. Ng, "Experimental Study of Reaction in a Partially-Wetted Catalytic Pellet," *AIChE J.*, **37**, 202 (1991).
Harold, M. P., "Steady-State Behavior of the Nonisothermal Partially-Wetted and Filled Catalyst," *Chem. Eng. Sci.*, **43**, 3197 (1988).
Harold, M. P., and K. M. Ng, "Effectiveness Enhancement and Reactant Depletion in a Partially Wetted Catalyst," *AIChE J.*, **33**, 1448 (1987).
Harold, M. P., P. Cini, B. Patenaude, and K. Venkataraman, "The Catalytically-Impregnated Ceramic Tube: an Alternative Multiphase Reactor," *AIChE Symp. Ser.*, **85**, 26 (1989).
Hatziantoniou, V., and B. Andersson, "Solid-Liquid Mass Transfer in Segmented Gas-Liquid Flow through a Capillary," *Ind. Eng. Chem. Fund.*, **21**, 451 (1982).
Hatziantoniou, V., and B. Andersson, "The Segmented Two Phase Flow Monolithic Catalyst Reactor: an Alternative for Liquid-Phase Hydrogenations," *Ind. Eng. Chem. Fund.*, **23**, 82 (1984).
Hatziantoniou, V., B. Andersson, and N. H. Schoon, "Mass Transfer and Selectivity in Liquid Phase Hydrogenation of Nitro Compounds in a Monolithic Catalyst Reactor with Segmented Gas-Liquid Flow," *Ind. Eng. Chem. Process Des. Dev.*, **25**, 964 (1986).
Herskowitz, M., S. Morita, and J. M. Smith, "Solubility of Hydrogen in α-Methylstyrene," *J. of Chem. and Eng. Data*, **23**, 227 (1978).
Ma, Y. H., "Effectiveness Factor in a Liquid-Filled Porous Catalyst," ScD Thesis, Massachusetts Institute of Technology," Cambridge (1967).
Madon, R. J., J. P. O'Connell, and M. Boudart, "Catalytic Hydrogenation of Cyclohexene: II. Liquid-Phase Reaction on Supported Platinum in a Gradientless Slurry Reactor," *AIChE J.*, **24**, 904 (1978).
Nguyen, M.-T., "Méthodologie D'Etude de Procédés à Catalyseur Suspendu," Doctoral Thesis, Ecole Nat. Sup. des Indus. Chim. de Nancy, France (1989).
Satterfield, C. N., A. A. Pelossof, and T. K. Sherwood, "Mass Transfer Limitations in a Trickle-Bed Reactor," *AIChE J.*, **15**, 229 (1969).
Turek, F., and R. Lange, "Mass Transfer in Trickle-Bed Reactors at Low Reynolds Number," *Chem. Eng. Sci.*, **36**, 569 (1980).
Watson, P. C. and M. P. Harold, "Exothermic Multiphase Reaction with Vaporization in the Single Catalytic Pellet: Modelling and Experiment," No. 126d, AIChE Meeting, Chicago (1990).
Yang, M. C., and E. L. Cussler, "A Hollow-Fiber Trickle-Bed Reactor," *AIChE J.*, **33**, 1754 (1987).

Appendix: Estimation of Temperature at the Gas-Liquid Interface

The heat flux Φ in the liquid-filled, active intraparticle region is given by:

$$\Phi = (T_{lb} - T)\,\frac{\lambda S}{(R_2 - R_1)} \tag{A1}$$

where R_1 and R_2 are the inside and outside radii of the tube, respectively; T_{lb} and T_2 are the liquid-phase temperatures in the bulk and at R_1, respectively; λ is the conductivity of AMS; and S is the exchange surface area. Φ is also equal to:

$$\Phi = h(T_2 - T_{gb})S \tag{A2}$$

where T_{gb} is the bulk gas-phase temperature, and h the heat transfer coefficient of hydrogen in laminar flow. By equating Eqs. A1 and A2, one can express T_2 as a function of the bulk gas- and liquid-phase temperatures:

$$T_2 = \frac{T_{lb}\lambda/(R_2 - R_1) + hT_{gb}}{H + \lambda/(R_2 - R_1)} \tag{A3}$$

The numerical value for λ is that of mesitylene at 20°C (0.136 W/K·m) and $R_2 - R_1 = 1$ mm. h was estimated to be equal to 224 W/K·m^2 (Bird et al., 1960).

Manuscript received Nov. 15, 1990, and revision received May 29, 1991.